IEEE Access
Multidisciplinary | Rapid Review | Open Access Journal

Received September 9, 2021, accepted September 18, 2021, date of publication September 22, 2021,
date of current version October 5, 2021.

Digital Object Identifier 10.1109/ACCESS.2021.3114763

Optimal Sizing of PV-Diesel-Battery System Using Different Inverter Types

ERICA M. OCAMPO, WEN-CHING CHANG, AND CHENG-CHIEN KUO
Department of Electrical Engineering, National Taiwan University of Science and Technology, Taipei 106335, Taiwan
Corresponding authors: Cheng-Chien Kuo (cckuo@mail.ntust.edu.tw) and Erica M. Ocampo (d10807802@gapps.ntust.edu.tw)

This work was supported by the Ministry of Science and Technology of the Republic of China under Grant MOST 110-3116-F-006-002.

ABSTRACT Different inverters types have different technical specifications and costs which contribute to the changes of inverter type decisions. It is therefore important to know which inverter is more advantageous for certain criteria. In this paper, the central, string, multi-string, and AC module types of inverters were compared through optimally designing a DG-PV and DG-PV-battery system of an off-grid island using each type of inverter. The problem was solved as a multi-objective optimization considering cost and uncertainty. The results were compared in terms of cost, reliability, renewable energy penetration, renewable energy curtailment, and changes in battery cost. The optimization results showed that the string inverter is best in terms of cost and highly affected by the decrease of the battery cost, the AC module in terms of reliability and curtailment, and the multi-string for renewable energy penetration. Meanwhile, the central inverter can be the choice when a balance between cost and reliability is considered.

INDEX TERMS Diesel generators, hybrid power system, inverters, optimal sizing, optimization, power generation planning, solar energy.

NOMENCLATURE

Unknowns

B	total battery system size (kW).
D	per unit diesel generator size (kW).
Inv	per unit inverter size (kW).
n_D	number of diesel generators.
n_{inv}	number of inverters.
S	total PV size (kW).

Constants

a, b	diesel generator fuel constants.
c_f	fuel cost.
$C_{I,INV}$	initial cost of inverter I.
$C_{I,x}$	initial cost of device x (diesel/PV/battery).
$C_{M,x}$	maintenance cost of device x (diesel/PV/battery).
df	minimum diesel generator demand factor.
ir	interest rate.
Irr	solar irradiation.
n	system life.
nr_x	number of replacements of device x.
η_{bat}	designated inverter for the battery.
η_{inv}	inverter efficiency.

Boolean

ch	battery charging state.
ds	battery discharging state.

Variables

C_I	initial cost.
C_M	maintenance cost.
C_R	replacement cost.
dQ	charge/discharge of the battery.
F	Fuel consumption (l/hr).
N_{Don}	number of diesel generators operating.
P^*	maximum power from a component.
P'_{inv}	minimum power from PV system.
P_{DG}	power generated by the diesel generator.
P^+_{DG}	power adjustment due to EMS.
P_{inv}	required power output from the PV system.
P^+_{inv}	power adjustment from PC system for battery charging.
P_L	power required by the load.
P_{PV}	generated power from the PV panels.
P_{sup}	required power for generation given the minimum required diesel generation.
Q	current charge on the battery.
Q_{max}/Q_{min}	max/min charge inside the battery.

The associate editor coordinating the review of this manuscript and approving it for publication was Qiuye Sun.

Economic Costs and Reliability Indices

ASC	Annual System Cost.
COE	Cost of Energy.
DEP	Dumped Energy Proportion.
LCOE	Levelized Cost of Energy.
LOLE	Loss of Load Expected.
LPSP	Loss of Power Supply Probability.
NPC	Net Present Cost.
RF	Renewable Factor.
TAC	Total Annual Cost.

Algorithms

BA	Bat Algorithm.
GA	Genetic Algorithm.
GOA	Grasshopper Optimization Algorithm.
GSA	Gravitational Search Algorithm.
GWO	Grey Wolf Optimization.
MFO	Moth-Flame Optimizer.
MOPSO	Multi-Objective Particle Swarm Optimization.
PSO	Particle Swarm Optimization.
SMO	Social Mimic Optimization.
SSA	Salp Swarm Algorithm.
SSO	Social Spider Optimization.
TLBO	Teaching and Learning Based Optimization.
WCA	Water Cycle Algorithm.
WOA	Whale Optimization Algorithm.

I. INTRODUCTION

The hybrid renewable energy system (HRES) model optimization solves for the most economic design of a hybrid combination of renewable and non-renewable energy sources for a given load profile. Combinations of wind, solar, and diesel generators (DG), in particular, are suitable for remote areas far from the main grid or in island locations. Wind energy does not provide many problems in system uncertainty, compared to photovoltaic(PV), because the loss of wind is aided by the inertia of the generators [1]. PV output, on the other hand, changes rapidly with the change in temperature or moving clouds [2]. That is why most HRES using PV usually have battery systems.

There are several papers that study the HRES model using PV for off-grid applications. Their focus varies on generator combination, renewable energy model, common bus system, objective function, and optimization method. Table 1 shows some studies in optimal sizing of HRES. Stand-alone PV focuses on optimal array-inverter configuration [3] and array selection [4] by minimizing the economic cost of the system. PV/DG combination is applied in [5] which considered the effect of load variation in peak and off-peak period in the sizing considering both total NPC and LPSP. Reference [6] determined the generator combination of wind-PV-battery minimizing the total cost for every given LPSP limit using GA-PSO as single-objective optimization and MOPSO as multi-objective optimization. Reference [7] studied the effects of tariffs using combinations of energy autonomy, power autonomy, capital cost, and payback period as objective functions to set a policy for a PV/battery/grid system sizing. Reference [8] uses the same combination of HRES to determine the effect of the pricing differences on the optimal combination of HRES. In [9], PV/DG/battery compared the designs for two types of batteries and two types of dispatch strategies using the HOMER software. Salameh *et al.* [10], likewise, used the HOMER software to study the costs of different types of solar trackers for the same combination of HRES systems. In [11] and [12], the focus was on the use of different algorithms in the sizing or a wind/PV/DG/battery system where both optimizations use the COE as their objective function. On the other hand, [13] and [14] approached the sizing of the same HRES as multi-objective but with fixed weights using both economic and reliability indices.

Most researches on HRES focused on a common DC coupling between the PV and the inverter because the inverter can be sized much smaller compared to the size of the PV because the excess energy can right away be stored in the battery. The size of the inverter is just enough to cater to the demand of the load with PV-inverter ratio usually range from 1.6 to 2.67 [3], [6], [8] for HRES combination with PV and can twice as much when a battery is added [6], [9]. On the other hand, researches in common AC coupling is scarce. It is only in [15]–[17] that considered a common AC bus between PV and battery. Though this configuration is not as economical as a common DC coupling, the common AC coupling is much more commonly seen as there are times that the PV plant and the BESS are in different locations or are handled by different operators. Reference [16] determined the optimal size of PV/DG/battery combination for a remote island in Canada. Reference [15] studied the best combination of renewable and non-renewable energy sizing while understanding the effects of load shifting on the costs for a residential power system. Reference [17] compared the use of time-sequence method, typical day method, and scenario reduction technique in the sizing of a wind/ PV/ DG/ battery system using TLBO.

Of the researches in Table 1, only a few researches [3], [6], [8], [9] considered the costs and configuration of the inverters of the PV. Inverters have an impact on the costs of the system and may even affect the size of HRES. Currently, there are four types of grid-connected inverter configuration, central, string, multi-string, and module-type inverters. In central inverters, the PV modules are connected in series for higher voltage, and these series modules are then connected in parallel for higher capacity making it the type of inverter with the highest available voltage and rating [18], [19]. These inverters are the cheapest type in the market, however, suffer from losses due to sting diodes, voltage mismatch, PV modules, and common MPPT causing failure for the PV plant because of the central inverter [19], [20]. String inverter, which is the most commonly used type of inverter, has a string of PV modules connected to a single inverter which makes it have a higher efficiency of 1-3% compared to the central

TABLE 1. Literature on optimal sizing of generators.

Reference	Bus System For PV-Batt	Sources	Objective/s	Optimization Method	Focus
Väisänen et al. (2019) [3]	(no battery)	PV	LCOE	-	Determine the optimal array-inverter ratio for every inverter size and tilt-angle for residential application
Zidane et al. (2019) [4]	(no battery)	PV	LCOE	GWO and SSA	Compare SSA and GWO; Compare two types of PV modules
Gharibi and Askarsadeh (2019) [5]	(no battery)	PV/DG	NPC and LPSP	MOPSO	Effect of load variation factor(in demand response) to the system sizing
Ghorbani et al. (2018) [6]	DC	Wind/PV/Battery	Total cost	GA-PSO and MOPSO	Optimal generation combination for the suburbs in Tehran, Iran given an allowed LPSP
Bandyopadhyay et al. (2020) [7]	DC	PV/Battery/Grid	Energy autonomy, power autonomy, capital cost, and payback period	MOPSO	Effect of tariffs on optimal sizing of the system
Ashtiani, et al. (2020) [8]	DC	PV/Battery/Grid	NPC and COE (single objective)	TLBO	Sizing for Iranian cities; compare pricing differences effect in renewable and non-renewable systems
Das and Zaman (2019) [9]	DC	PV/DG/Battery	NPC	HOMER	Compares two types of batteries and two types of dispatch strategies
Salameh, et al. (2020) [10]	DC	PV/DG/Battery	NPC	HOMER	For a microgrid in UAE; compare single-axis and dual-axis trackers
Bukar, Tan, and Lau (2019) [11]	DC	Wind/PV/ DG/Battery	COE	GOA, CS, and PSO	Sizing for a microgrid in Nigeria;
Daib, et al. (2019) [13]	DC	Wind/PV/ DG/Battery	COE, LPSP, and Loss (fixed weights)	WOA, WCA, MFO, and PSO-GSA	Sizing for a microgrid in Egypt
Fathy, Kaniche and Alanazi (2020) [12]	DC	Wind/PV/ DG/Battery	COE	SSO	Compare SSO with other algorithms; sizing and combination of energy sources for a region in Saudi Arabia
Mohammed, Al-Anbarri and Hannun (2020) [14]	DC	Wind/PV/ DG/Battery	LCOE and LOLE (fixed weights)	PSO, BA, SMO	A novel demand response strategy for the battery; comparison of PSO, BA, and SMO
Nejabatkhah et al. (2018) [16]	AC	PV/DG/Battery	ASC	MATLAB	Sizing for a remote off-grid in Canada
Akram, Khalid, and Shariq (2018) [15]	AC	Wind/PV/ DG/ Battery	Total of economic, dump energy and emission costs	-	Combination and sizing of generators; load shifting effect
Yang, et al. (2019) [17]	AC	Wind/PV/ DG/Battery	TAC (with RF, LPSP and DEP limits)	TLBO	Use of k-means based scenario reduction technique compared with typical day method and time-sequence simulation

inverter type due to some diode losses eliminated and individual MPPT applied in every string [18], [20]. However, string inverter types only have power ratings up to 10kW per string, thus, needing more inverters for higher PV plant capacity. The multi-string inverter has each PV module string connected to a DC-DC converter whose output is connected to the input of a common inverter. This makes multi-string is a hybrid of the central and the string types because each string can be controlled and monitored individually, has MPPT for every string, allows strings of different technologies but can be unreliable due to a common inverter [18]–[20]. Lastly, the module-type inverter or most commonly known as micro-inverter has an inverter connected to each PV module which makes this type have the least losses, longer life, individual module failure detection, easier to expand, and deals with partial shading. On the other hand, the module type has reduced overall efficiency, high cost per kilowatt, low power output, and higher amplification [18]–[20].

Generally, each type of inverter has a different available rating range, efficiency, life span, and cost which can contribute to the decision-making for system sizing. In literature, only the paper of Tariq *et al.* [21] compares the different types of inverters. In their paper, the reliability of the PV system in terms of failure rates of both the PV modules and inverters (central, string, and micro-inverter) were studied using the bathtub cycle, which includes an infant period, useful period, and wear-out period for every inverter replacement. However, it only studies the effect of the performance of the inverters on the life-cycle costs of the system. Though the NREL report in [22] showed the costs of using different inverters, the focus was providing the costs of common inverters used for each industry based on a benchmark system for system

per industry. In an island system, the type of consumers is an amalgam of loads and may be too small to be compared to the utility scale mentioned in the report. It is, therefore, important to know the differences of using this type of set-up.

This paper studies the applications of different inverter types in a DG-PV and DG-PV-battery system by considering economy and uncertainty, as a multi-objective optimization. In this way, it may help system designers to not only decide on the equipment sizing but also in choosing the type of inverter.

The limitation of this paper is that the energy management strategy (EMS) involves a rule-based strategy commonly used in sizing problems, as presented in [13], [17], [23]. However, for future research, it can be recommended to try either other rule-based strategies such as cycle charging [10], [16], co-optimization to simultaneously solve generation and power dispatch [24], state-space approaches (model predictive) to control [25], or stochastic approaches to control [26].

This paper is organized as follows. Section 2 discusses the models for the DG, PV, battery, and the charging-discharging strategy for the battery. The multi-objective problem is explained in section 3 followed by the discussion on the optimization method used. The results and discussion are presented in section 4. Further discussion and summary of the results are discussed in section 5. Finally, Section 6 is the conclusion.

II. SYSTEM MODEL

Figure 1 shows the system being studied with DG as the main energy source connected to an AC bus providing AC loads. For this study, it would be required for at least one DG to be operating to maintain the frequency of the system.

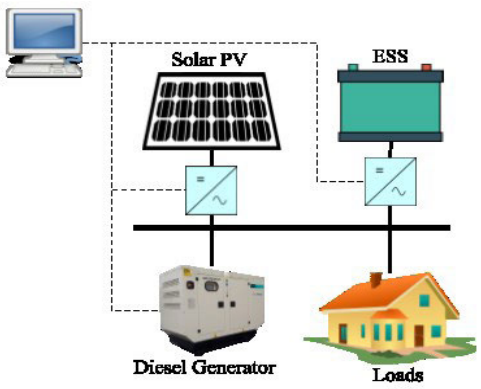

FIGURE 1. Simplified hybrid PV/diesel/battery system.

A. DIESEL GENERATORS

The diesel generators of the same sizes D are used for the system and are computed as follows:

$$F(t) = a \cdot P_{DG}(t) + b \cdot D \cdot N_{on}^{D}(t) \quad (1)$$

The a and b constants used are 0.246 and 0.08145 taken from [11], [13], [23]. Equation (1) shows a modified equation from literature since this system allows some generators to turn off when the load is not too high. Instead of multiplying the second term by the state of the generator, it is multiplied by the total number of operating generators N_{on}^{D} at a time (t).

B. PV SYSTEMS

For this particular problem, the 3-year hourly irradiation data are taken from SoDa [27]. Using the Gaussian distribution, an hourly solar irradiance was modeled from the average of the 1-year daily irradiation, as shown in Figure 2.

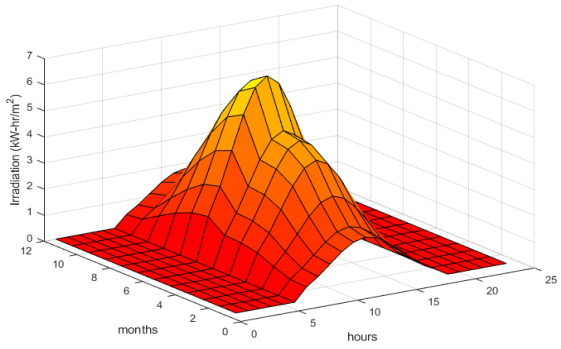

FIGURE 2. Average hourly irradiation per month.

The power output of the PV and the inverter is then computed as (3), as adopted from [28]. $P_{PV}(t)$ is the output of the PV panels per at each hour, P_{inv} is the output of the inverter at each hour and n_{inv} is the number of inverters used. N_{pv} and N_{inv} are the efficiencies of the available PV panel and inverter, respectively.

$$P_{PV}(t) = S \times Irr(t)/Irr_{max} \quad (2)$$

Another set of one-year solar irradiation profile, Figure 3, was made to represent the uncertainty of the irradiation based on data taken from SoDa. This incorporates the variation of the irradiation based on the data's daily distribution for each month.

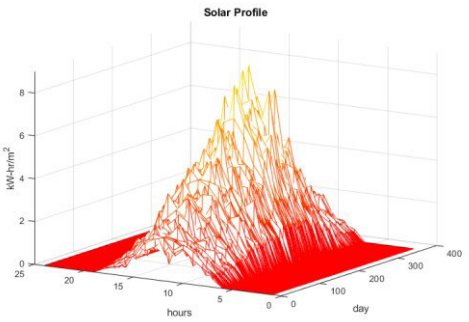

FIGURE 3. One-year solar irradiation (with uncertainty).

C. BATTERY AND ENERGY MANAGEMENT SCHEME

The energy management strategy (EMS) used in [13], [17], [23] was modified to include requiring at least one diesel

generator to maintain the system frequency. The EMS handles most of the power flow constraints, such as power limit for the PD, PV, and charge of the battery, and charging-discharging conditions. As shown in equation (3), the P_{sup} is equal to the load P_L minus the power generated by one diesel generator working at its minimum demand factor *df*. The additional required generation P_{sup} shall then be supplied first by the PV plant P'_{inv} if the power is available from the output of the inverter (4), followed by the available charge from the battery (condition 2 of equation (5)), and finally the additional power from the diesel generators P_{DG+} in (8). The total power generated by the diesel generators (9) will then be the sum of one diesel generator operating at minimum df and the additional power P_{DG+}.

The batteries are charged when there is excess generation from the PV Pinv+, as shown in the first condition in (5) indicated by the negative sign for dQ and (7). The final power output from the PV plant (10), on the other hand, is the sum of the available power from the PV plant to be supplied to the load P'inv and the power needed to charge the battery Pinv+. ηinv and ηbat are the PV inverter efficiency and the battery inverter/converter efficiency.

$$P_{sup}(t) = P_L(t) - df * D \tag{3}$$

$$P'_{inv}(t) = min\left(P_L(t) - df * D, \eta_{inv}P_{PV}(t)\right) \tag{4}$$

$$\begin{aligned} if\ ch &= \left(\eta_{inv}P_{PV}(t) \geq P'_{inv}(t)\right) is\ true \\ dQ(t) &= -max\left(min\left(Q_{max} - Q(t-1), \right.\right. \\ &\quad \left.\left. \times \frac{\left(\eta_{inv}P_{PV}(t) - P'_{inv}(t)\right)}{\eta_{bat}}\right), 0\right) \\ if\ ds &= \left(P_{sup}(t) > \eta_{inv}P_{PV}(t)\right) \& \left(Q(t-1) > Q_{min}\right) \\ &\quad \times is\ true \\ dQ(t) &= max\left(min\left(Q(t-1) - Q_{min}, \right.\right. \\ &\quad \left.\left. \times \left(P_{sup}(t) - \eta_{inv}P_{PV}(t)\right)/\eta_{bat}\right), 0\right) \end{aligned} \tag{5}$$

$$Q(t) = Q(t-1) + dQ(t) \tag{6}$$

$$P_{inv+}(t) = -ch * \eta_{bat}dQ(t) \tag{7}$$

$$P_{DG+}(t) = P_{sup}(t) - ds * \eta_{bat}dQ(t) - P'_{inv}(t) \tag{8}$$

$$P_{DG}(t) = df * D + P_{DG+}(t) \quad \text{if } P_{DG+} \text{ is } (+) \tag{9}$$

$$P_{inv}(t) = P'_{inv}(t) + P_{inv+}(t) \quad \text{if } P_{inv+} \text{ is } (+) \tag{10}$$

III. PROBLEM FORMULATION

The two objective functions used in this study are the COE and the LPSP which represent the cost and reliability considerations for this system.

A. ECONOMIC MODEL

The equations for the NPC, COE, and LPSP are shown in (11), (12), and (13), respectively. The investment cost, maintenance cost, operation cost, and replacement cost are computed as shown in (14), (15), (16), and (17), respectively. The number of replacements and devices for either the diesel generator, inverter, or battery is computed in (18) and (19), respectively.

$$NPC = (C_I + C_M + C_O + C_R) / \left(\frac{i(1+i)^n}{(1+i)-1}\right) \tag{11}$$

$$COE = \frac{NPC}{totalLoad} \tag{12}$$

$$LPSP = \frac{\left(\sum_{t=1}^{8760} P_L(t) - P_D(t) - P_{INV}(t) - P_{Batt}(t)\right)}{\sum_{t=1}^{8760} P_L(t)} \tag{13}$$

$$C_I = n_D D \cdot C_D + S \cdot C_{PV} + n_{INV} INV \cdot C^i_{INV} + B \cdot C_{Batt} \tag{14}$$

$$C_M = \left(n_D \cdot D \cdot C_{M,D} + S \cdot C_{M,PV} + B \cdot C_{M,Batt}\right) \tag{15}$$

$$C_O = \left(\sum_{t=1}^{8760} c_f F_D(t)\right) \tag{16}$$

$$C_R = nr_D n_D C_{I,D} + nr_{INV} n_{INV} C_{I,INV} + nr_B n_B C_{I,B} \tag{17}$$

$$nr_{device} = \left\lceil \frac{\text{system life}}{\text{life of a component}} \right\rceil - 1 \tag{18}$$

$$n_{device} = \left\lceil \frac{P^*_{device}}{\text{Rating}_{device}} \right\rceil \tag{19}$$

The different constants used are found in Tables 2 and 3. The values in Table 2 are based on the descriptions in literature [11], [18], [20] and available inverter specifications in the market.

TABLE 2. Technical and economic specifications for inverters.

	Initial costs ($ /kW)	Life	Efficiency	Sizes (kW)
Central Inverter	140	5 years	95 %	30-5000
String Inverter	383	10 years	96 %	1-5
Multi-String	452	8 years	97 %	10-50
AC Module	900	25 year	97.5%	0.5

TABLE 3. Technical and economic specifications.

PV		
Initial cost	2900	$/kW
Maintenance	16	$/kw/yr
Life	25	yrs
Efficiency	95%	
Diesel		
Initial cost	1000	$/kW
Maintenance	0.05	$/hr
Operation	0.9	$/l
a and b constants	0.246 and 0.08145	
Life	24000	hrs
Min demand factor	40%	
Battery		
Initial cost	280	$/kWh
Maintenance	10	$/kWh/yr
Life	12	yr
Efficiency	85	%
Economic		
Interest Rate	13	%
Discount Rate	8	%

B. COMPARATIVE INDICES

There are three indices to be studied in this paper, PV-inverter ratio, renewable energy penetration (%RE), and

RE curtailment. For clarity, these terms will be defined in this subsection.

PV-inverter ratio will be referred to as the size ratio of the PV system. This would be the ratio of the total size of PV to the total size of inverters.

Renewable energy penetration is the percentage of RE present in the system that carries the load. RE curtailment on the other hand is the percentage of curtailed energy from the RE source.

$$\%RE = \frac{\sum P_{inv}}{\sum P_L} \times 100\% \tag{20}$$

$$RE\ curtailed = \frac{\sum \eta_{inv} P_{PV} - P_{inv}}{\sum \eta_{inv} P_{PV}} \times 100\% \tag{21}$$

C. OPTIMIZATION APPROACH

The multi-objective problem (22) was initially solved as a single objective problem by setting the weight to 1 and 0, thereby, giving the results for the least COE (f_1) and least LPSP (f_2), respectively. This is followed by varying the value of the weight from 0.05 to 0.95 to get the Pareto front.

$$f(f_1, f_2) = \omega \left(\frac{f_1(x) - f_{1min}}{f_{1max} - f_{1min}} \right) + (1 - \omega) \left(\frac{f_2(x) - f_{2min}}{f_{2max} - f_{2min}} \right) \tag{22}$$

After getting the Pareto fronts for the different systems with different inverters. The optimal point or optimal design was determined using (23). Note that this is the normalized distance to the utopia point for multi-objective optimization.

$$f(f_1, f_2) = \sqrt{\left(\frac{f_1(x) - f_{1min}}{f_{1max} - f_{1min}} \right)^2 + \left(\frac{f_2(x) - f_{2min}}{f_{2max} - f_{2min}} \right)^2} \tag{23}$$

GA and PSPSO [19] algorithms (N = 50, maximum iterations = 1000) were used to optimize (22) while varying the weight ω. The result with better minimized result was chosen as the solution. Though the results of the two algorithms were compared, the simulation shows that the PSPSO always gives better results.

D. SYSTEM ASSUMPTIONS

In this case study, a one-year load, and solar irradiation profiles for a Taiwan setting are used for the general design of the system. The uncertainty profile was later on used to analyze a possible scenario during the operation of the system, which values reflect on the computation of the LPSP, as shown in Figure 4 fitness evaluation. The output of PV (2) is recomputed followed by an adjustment in the EMS.

Since the system uses an island condition, where loads are mostly residential and power lines do not need to travel long distances, a steady-state condition is considered, using only real power and without considering line losses.

Additionally, the power balance equation is not directly included in the constraints as excess energy is reflected in the cost of producing more energy while insufficient energy reduces the reliability of the system. Inclusion of the power balance, with the losses and excess energy, will be redundant to the EMS which already sets the rule of the energy flow in the system.

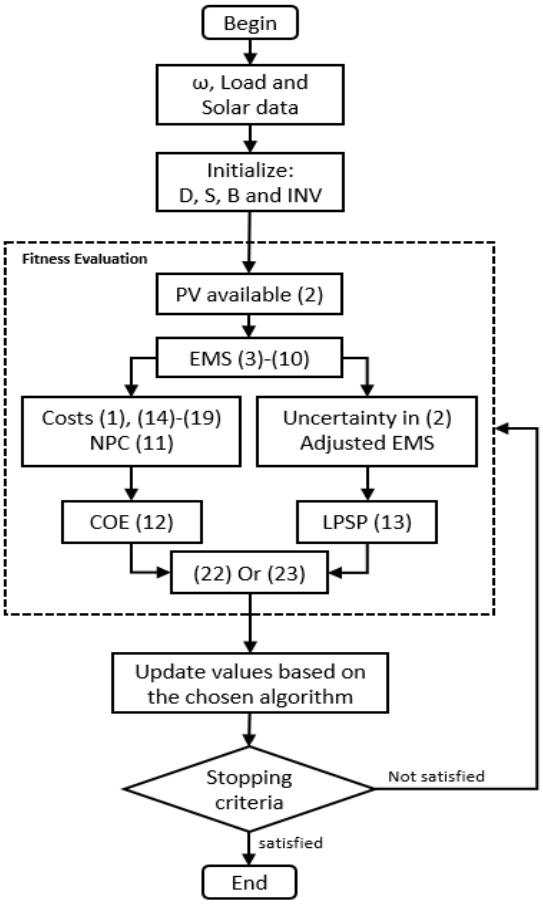

FIGURE 4. Optimization flowchar.

IV. RESULTS

The problem was solved using MATLAB using both GA and PSPSO [29] as the optimization algorithms with the optimization scheme shown in Figure 4. Because the focus of this paper is not the optimization algorithm, the problem was solved by running the problem several times on both algorithms. The result with the least objective function was chosen as the result.

A. SINGLE OBJECTIVE APPROACH

Using the same problem as above, the design for minimum COE and LPSP were optimized separately to determine the minimum and maximum limits for each type of inverter. Table 4 shows the design for each system using different inverters for least COE and least LPSP for DG/PV and DG/PV/battery systems.

For a diesel generator the only system, the optimal design has a COE of 0.0642. It can be seen with the least COE that with the PV, the cost of the system decreases for all except for the central type inverter. This may be due to the smallest size

TABLE 4. Optimal results for least COE and least LPSP.

System	Obj.	Inverter Type	Diesel (kW)	Total Diesel (kW)	Total PV (kW)	Total Battery (kW)	Inv (kW)	Total Inv (kW)	COE ($/kW)	LPSP
DG only	COE	DG only	11	484	-	-	-	-	0.0642	0
DG-PV	least COE	Central	19	475	30	-	30.00	30.00	0.0649	1.23E-15
		String	19	475	1	-	1.00	1.00	0.0632	1.18E-15
		Multi-string	19	475	10	-	10.00	10.00	0.0638	1.22E-15
		AC Module	19	475	1	-	0.50	0.50	0.0632	1.16E-15
	least LPSP	Central	76	532	1420	-	545.00	545.00	0.1313	7.83E-17
		String	76	532	1420	-	5.00	430.00	0.1334	7.93E-17
		Multi-string	71	497	1397	-	17.00	442.00	0.1394	8.62E-17
		AC Module	76	532	1359	-	0.50	426.50	0.1445	8.60E-17
DG-PV-Batt	least COE	Central	19	475	30	1.00	30.00	30.00	0.0649	1.23E-15
		String	19	475	1	1.00	1.00	1.00	0.0632	1.18E-15
		Multi-string	19	475	10	1.00	10.00	10.00	0.0638	1.22E-15
		AC Module	19	475	1	1.00	0.50	0.50	0.0632	1.16E-15
	least LPSP	Central	71	497	1420	25.00	636.00	636.00	0.1403	9.09E-17
		String	76	532	1420	25.00	4.00	448.00	0.1346	9.44E-17
		Multi-string	61	488	1397	25.00	50.00	500.00	0.1383	9.59E-17
		AC Module	61	488	1359	25.85	0.5	453.56	0.1553	1.01E-16

of this inverter may be too large for the system. The string and AC module have the lowest cost followed by the multi-string and central type inverters. When the LPSP is prioritized, the central type of inverter has the lowest, followed by the string inverter, AC module, and multi-string.

For a system with batteries, when COE is prioritized, the same values for CEOs can be seen even with the smallest size of the battery. However, these values are still cheaper than a DG-only system. When the LPSP is prioritized, the central type again has the lowest LPSP.

For the diesel sizing, the per-unit size and total size increase when LPSP was considered. This is due to the system prioritizing the diesel when uncertainty is considered. When the battery is added, most of the total sizes increases, except for the central inverter type.

PV sizing likewise increases when LPSP is considered, and slightly decreases when the battery was added. Note that for the least COE, the per-unit size of PV uses about the same size as the inverter. Same as the diesel generators, the per-unit size and total size of inverters increases when LPSP is considered. When the battery was added, per unit size and total size of inverters generally increase also.

For both the DG-PV and DG-PV-battery systems, the systems with inverter types giving the least COE are the string type while the lowest LPSP is the central type.

Table 5 shows the information for the RE system. Generally, when considering the least COE, the PV-inverter ratio is around 1. This ratio increases to around 3 when the LPSP is considered with the largest of 3.302 for the string type. This ratio decreases slightly when the battery is added. It can also be seen for both the DG-PV and the DG-PV-battery systems, the central inverter has the lowest ratio while the string has the highest ratio.

The RE penetration increases when the LPSP is considered but decreases when CEO is considered. It can be said that the maximum penetration of RE can be around 42% for the PV/DG system and 44% when the battery is added. The inverter with the highest RE penetration is the multi-string type for most cases. On the other hand, the system with the string type, in almost all cases, has the lowest RE penetration followed by the multi-string.

TABLE 5. RE information for least LPSP and COE.

System	Obj.	Inverter Type	PV: INV	%RE	RE curtailment (%)
DG-PV	least COE	Central	1.000	1.63	0.00%
		String	1.000	0.05	0.00%
		Multi-string	1.000	0.55	0.00%
		AC Module	1.000	0.03	0.00%
	least LPSP	Central	2.606	42.43	81.76%
		String	3.302	42.57	83.07%
		Multi-string	3.161	42.75	81.21%
		AC Module	3.185	42.19	79.49%
DG-PV-Batt	least COE	Central	1.000	1.63	0.00%
		String	1.000	0.05	0.00%
		Multi-string	1.000	0.55	0.00%
		AC Module	1.000	0.03	0.00%
	least LPSP	Central	2.233	43.53	77.15%
		String	3.170	43.42	79.48%
		Multi-string	2.794	44.10	75.65%
		AC Module	2.995	43.81	72.86%

When COE is considered, there is no RE curtailment in the system. This means that all generated power from RE was used. On the other hand, very large curtailment is seen for all systems when only the LPSP is considered. This is due to the oversizing of the PV compared to the inverter to lessen the uncertainty from RE leading to large curtailment. However, this curtailment decreases when batteries are included in the system. Using AC module type inverter gives the lowest curtailment in both systems while the systems using the string and the central type inverters give the highest curtailment.

B. MULTI-OBJECTIVE APPROACH

1) PARETO FRONT

The Pareto front of the DG-PV system and DG-PV-battery system for different types of inverters are shown in Figure 5,

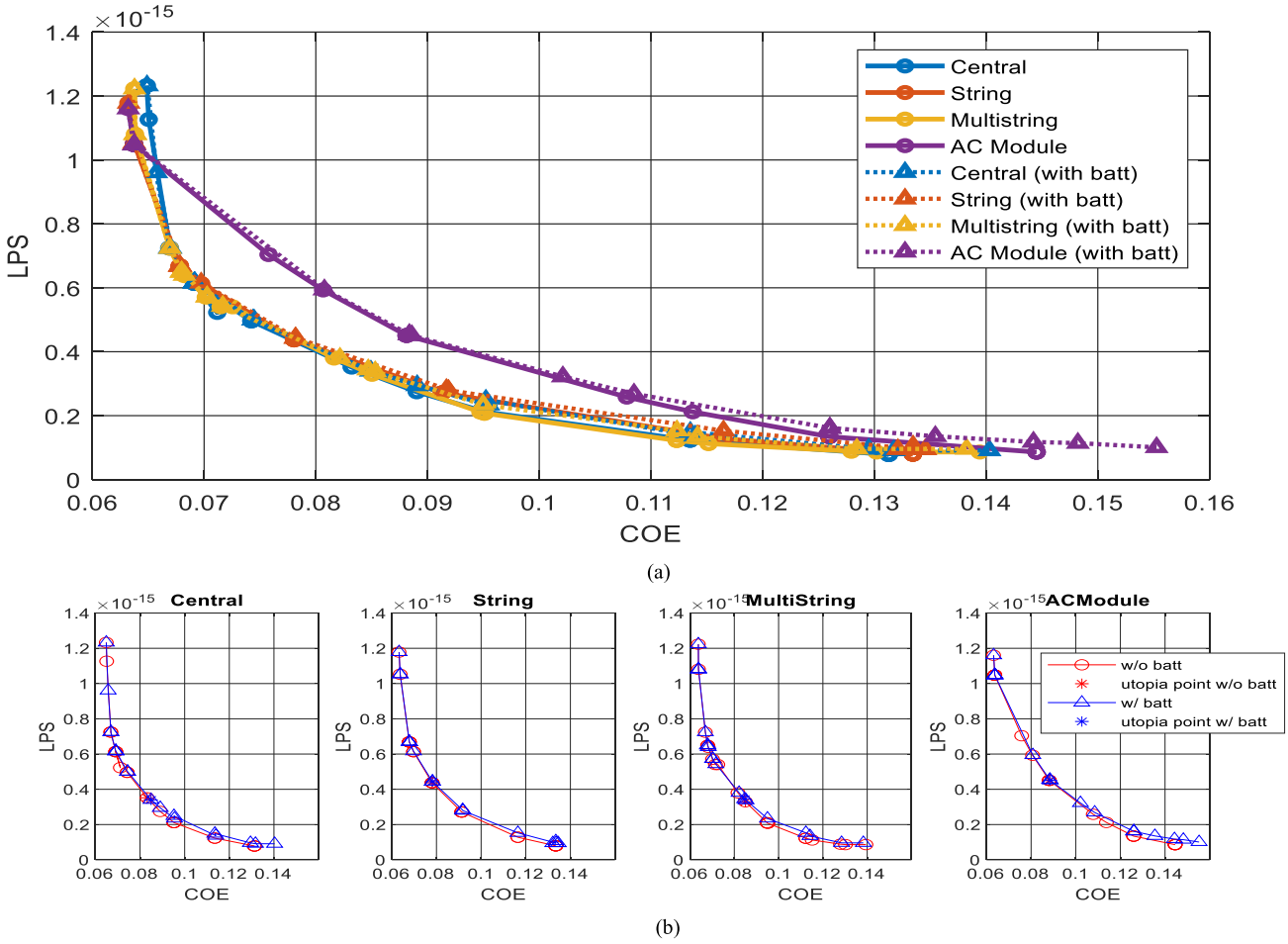

FIGURE 5. Pareto fronts of DG-PV system and DG-PV-battery system for all inverter types (a) combined in one figure and (b) taking each one separately with row 1 as the PV-DG system and row 2 is the PV-DG-battery system. The optimal result for each type of system is marked with a (*).

with the combined figures in Figure 5(a) and separated figures but with the same axes in Figure 5(b).

Notice that for all types of inverter with their respective systems, the results to the left of the utopia point is almost collinear. It can also be seen that at these segments, the COE and LPSP values with the same weights lie on almost the same point. This means that when the COE is prioritized, the design of the system with the battery is as competitive as the design of the system without the battery until it reaches its optimal point. The difference between the costs and reliability would be seen when the LPSP is prioritized, as the branching of the Pareto front is seen to the right of the optimal point.

As the central inverter may be the most expensive when the cost is prioritized, its Pareto front can be nearer to the utopia point when there is more balance between cost and reliability. To the right of the optimal point, the costs increase more for the system with the battery as the LPSP is prioritized compared to the system without the battery.

The system with the string inverter has cheaper when the cost is prioritized compared to the system with the central inverter. We can also see that each point of the Pareto front for both the PV-DG and PV-DG-battery systems using the string inverter are very near each other compared with other inverters. The points to the right of the optimal point shift up for the system with the battery when the LPSP is prioritized, meaning that there is an increased LPSP when the battery is included but with the same cost.

For the multi-string, the characteristic is somehow similar to both the central and the string inverters in a way that it almost has the same range of LPSP and COE but extends for both DG-PV and DG-PV-battery like the string inverter. Also, like the string inverter, the system with the battery has an increased LPSP with the same cost.

Unlike the other inverters, the slope of the Pareto front of the AC module is much straighter compared to the other inverters. This means that the cost is largely affected by the reliability of the system. The cost extends further when the LPSP is prioritized past the optimal point.

2) SYSTEM SIZING

Table 6 shows the results for the optimal points, determined using equation (23), wherein the chosen optimal points all lean to the reliability. All weights for COE for the DG/PV

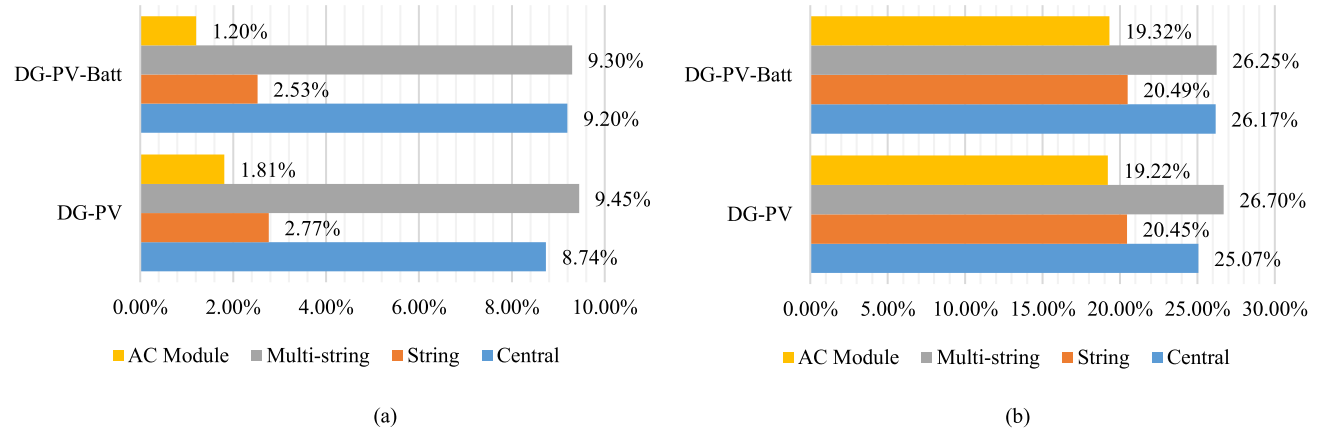

FIGURE 6. (a) Percentage of RE curtailed and (b) percent penetration of RE (%RE) in the system of the optimal result in Table 6.

TABLE 6. Optimal result for different inverters and systems.

System	Inverter Type	Diesel (kW)	Total Diesel (kW)	Total PV (kW)	Total Battery (kW)	Inv (kW)	Total Inv (kW)	PV: INV	COE ($/kW)	LPSP	Weight of COE
DG-PV	Central	61	488	502	-	446	446	1.126	0.0832	3.52E-16	0.45
	String	41	492	383	-	5	345	1.110	0.0781	4.37E-16	0.45
	Multistring	41	492	527	-	50	450	1.171	0.0850	3.29E-16	0.45
	AC Module	41	492	351	-	0.5	342.5	1.025	0.0881	4.51E-16	0.45
DG-PV-Batt	Central	61	488	527	13	253	506	1.042	0.0849	3.40E-16	0.4
	String	41	492	383	6	5	350	1.094	0.0782	4.43E-16	0.4
	Multistring	61	488	518	13	48	432	1.199	0.0847	3.44E-16	0.3
	AC Module	41	492	351	25	0.5	343	1.025	0.0886	4.51E-16	0.45

system are 0.45, while for the DG-PV-battery system range from 0.3 to 0.45. As discussed in the previous section, the optimal points (value of COE and LPSP) for both DG-PV and DG-PV-battery systems are almost the same for their corresponding inverter type.

The DG-PV and DG-PV-battery systems using the central inverter uses the same size as diesel generators. The total PV size and inverter size can be increased when batteries are included in the system.

For the string type inverter, both the DG-PV and DG-PV-battery have the same size as DG and PV. The inverter size increased a little when the batteries were included in the system.

The multi-string type is the only inverter type with the decrease in DG size, PV size, and inverter size when the battery is considered. It is also the only inverter type with a decrease in COE.

Lastly, the AC module has the same size for the DG, PV, and inverter for both DG-PV and DG-PV-battery systems.

Figure 6 shows the summary on RE curtailment and RE penetration for each inverter type for the DG-PV and DG-PV-battery systems. The central inverter type has one of the highest RE penetration and can further increase when a battery is included in the system. However, the increase in penetration also increases the curtailment. The string inverter has one of the lowest RE penetration. Even with the addition of the battery, the RE penetration for the string inverter increases by just a little. On the other hand, it has one of the lowest curtailments. The multi-string module has the highest RE curtailment and at the same time the highest RE penetration for both types of systems. The addition of the battery slightly decreases both the penetration and the curtailment. Lastly, the AC module has the lowest curtailment and the lowest RE penetration.

Figure 7 shows the power flow on the day with maximum and minimum load for the DG-PV system (Fig 7(a)) and DG-PV-battery system (Fig.7(b)). The day with maximum load occurs during the summertime where the output from the PV is also high while the day with the minimum load occurs during the wintertime where the output of the PV is low. Note that during the wintertime, the climate in Taiwan is not that cold to use heaters.

In Figure 7(a), the designs using the central and the multi-string inverters are quite large as seen on the day with maximum load making it curtail much RE especially during the sudden drop of load during the 11th to the 13th hours, which is the "lunch" hours. The systems using the string and the AC module, on the other hand, have a peak PV output lower than the maximum load during the day with maximum load, almost no PV curtailment is seen and the DG has lesser hours operating at minimum load. For the day with minimum load, all the generated PV were used for all types of inverters, with all the DGs operating above their minimum load.

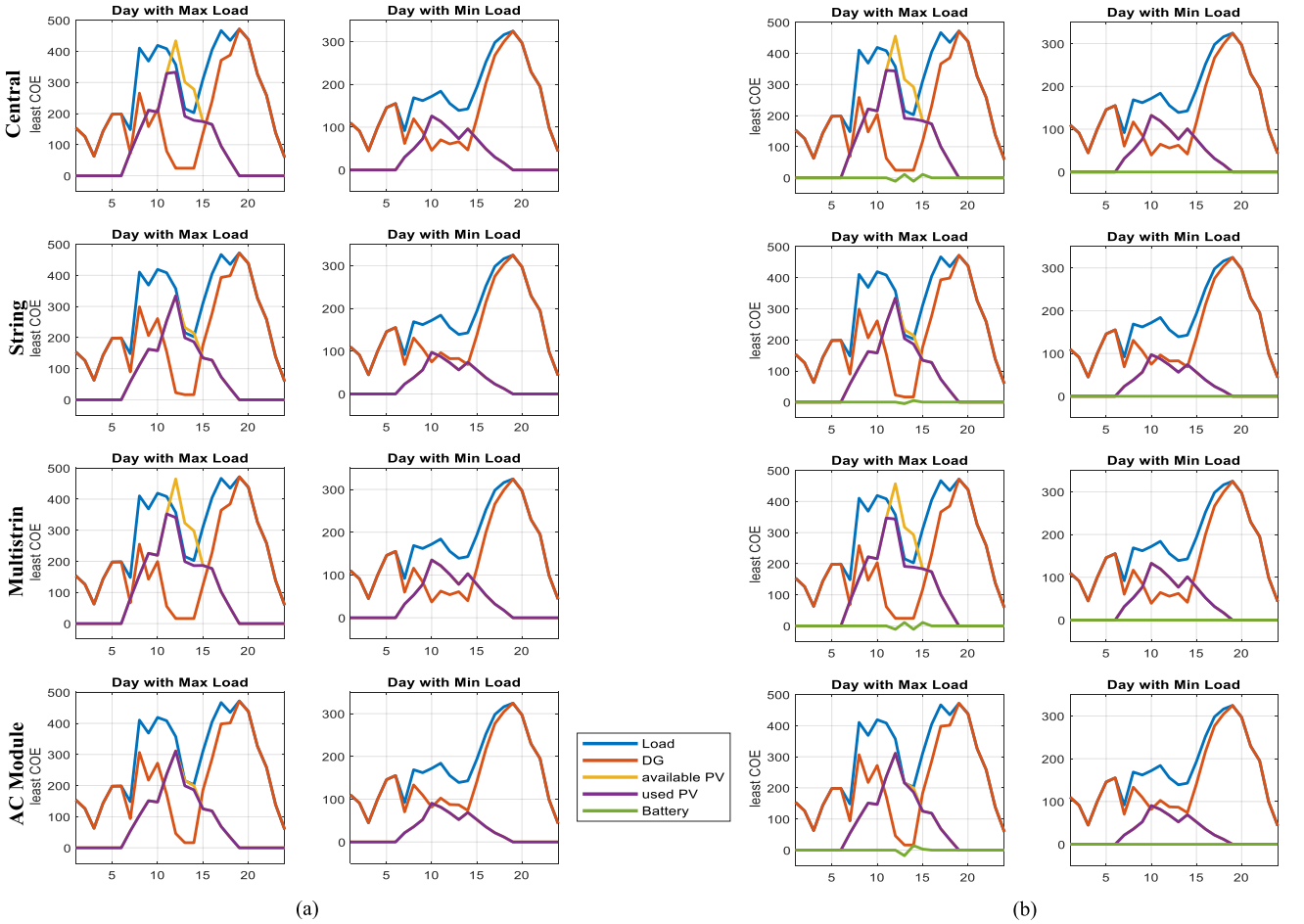

FIGURE 7. Power flow for the day with maximum load and minimum load for the (a) DG-PV system and (b) DG-PV-battery system.

For Figure 7(b), it can be seen that the design using the central type inverter is larger compared to its system with no battery. This is the reason why there is an increased RE curtailment for its system with the battery on the hours where there is a decrease in load. Even though the battery uses the extra energy from the PV to charge, the battery easily gets fully charged and assists the PV in the dispatch during the ''lunch'' hours to prevent the system from taking power from the DGs. After which, the battery charges and discharges again. This is also true for the system using the multi-string inverter but this time with some decrease in total PV size compared to its DG-PV system. The string and the AC module have the same size of DG and PV with the addition of the battery that is sufficient enough to decrease the RE curtailment during the ''lunch'' hours.

3) ANALYSIS ON FUTURE COST REDUCTION ON BATTERIES

In a study of NREL [30], the projection of battery prices is expected to drop in the next year by 20% and in five years by 50%. This effect is studied in this section to study the cost-benefit in differing the commissioning of the HRES with battery.

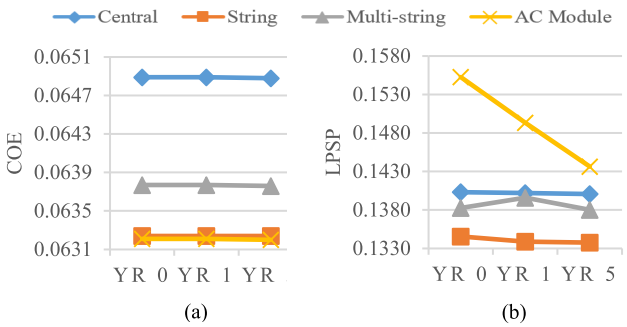

FIGURE 8. Effect of projected battery prices on COE based on (a) least COE and (b) least LPSP decision.

Figure 8 (a) and (b) shows the effects of this reduced cost on the COE for the least COE and least LPSP decisions. The results of the LPSP are not shown because it did not change from year 0 to year 5. Also, the resulting sizes of the DG, PV, and battery remain the same from year 0 to year 5. The results for the least COE decision show (Figure 8-a) that the effect of the price of the battery is not much affected as the size of

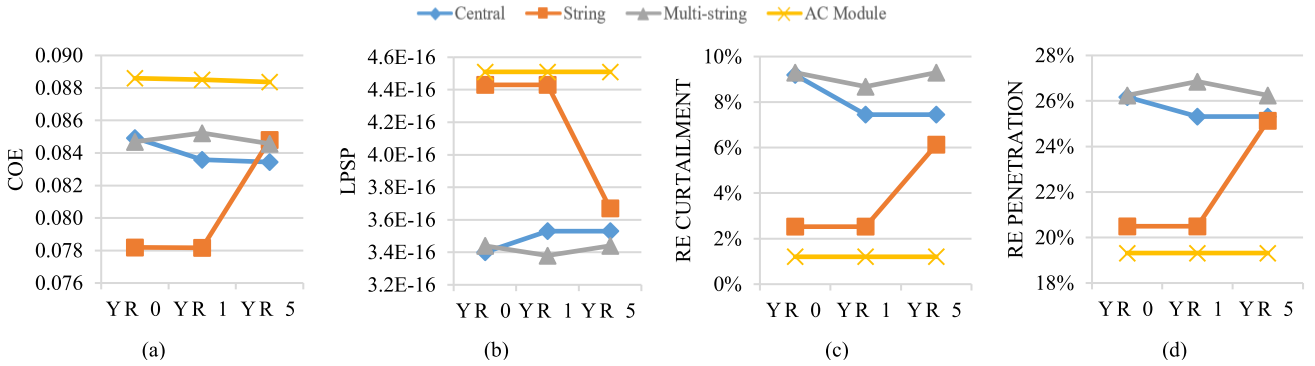

FIGURE 9. Effect of projected battery prices on the optimal result: (a) COE, (b) LPSP, (c) RE curtailment and (d) RE penetration.

TABLE 7. Optimal results (multi-objective) for decrease in cost of batteries.

Year	Inverter Type	Diesel (kW)	Total Diesel (kW)	Total PV (kW)	Total Battery (kW)	Inv (kW)	Total Inv (kW)	COE ($/kW)	LPSP
Year 0	Central	61	488	527	13	253	506	0.0849	3.40E-16
	String	41	492	383	6	5	350	0.0782	4.43E-16
	Multi-string	61	488	518	13	48	432	0.0847	3.44E-16
	AC Module	41	492	351	25	0.5	343	0.0886	4.51E-16
Year 1	Central	61	488	502	25	449	449	0.0836	3.53E-16
	String	41	492	383	6	5	350	0.0782	4.43E-16
	Multi-string	41	492	527	13	50	450	0.0852	3.38E-16
	AC Module	41	492	351	25	0.5	343	0.0885	4.51E-16
Year 5	Central	61	488	502	25	474	474	0.0834	3.53E-16
	String	41	492	487	25	5	435	0.0848	3.67E-16
	Multi-string	61	488	518	13	50	450	0.0846	3.44E-16
	AC Module	41	492	351	25	0.5	343	0.0884	4.51E-16

the RE is small. When the least LPSP is used (Figure 8-b), the effect of this change can be greatly seen for the design using the AC module with a decrease in COE of 3.81% for year 1 and 7.48% for year 5.

Figure 9 shows the changes for the optimal results. Again, the COE for the design using the AC module can be seen affected by the change in battery prices. Even though the decrease in COE for the string module is small, the LPSP and RE penetration improve appreciably. The LPSP decreases by 17.16% while the penetration increases by 22.63%. This also corresponds to an increase in curtailment for the string inverter. The results for the sizes of the optimal results can be seen in Table 7 and we can verify that the resulting system size for the string inverter can be comparable now to the sizes of the system with the central and the multi-string.

V. DISCUSSION

From the results above, several recommendations can be made for each criterion:

- For the least cost, the string inverter can be recommended for both DG-PV and DG-PV-battery systems.
- For least LPSP, the AC module can be used. However, when the battery is available, an advantage on both the cost and reliability can be seen for the central over other types.
- The highest penetration can be seen using the multi-string inverter in both single objective and multi-objective results of both systems.
- The AC module always has the lowest curtailment of energy.
- The decrease in the cost of the battery improves greatly the reliability of the AC module when the reliability is only considered.
- When considering both cost and reliability, the string type is affected the most when the cost of the battery is decreased. Though initially, it has the lowest cost, its cost increases after the increase of the battery size, which improves the reliability, curtailment, and increases RE penetration.

From these results, we can therefore summarize the use of each type of inverter as follows:

- The central inverter has the nearest to utopia point between the four inverters and can be therefore be used when a balance between cost and reliability is considered.
- The string inverter has the lowest COE and is highly affected by the change in battery cost.
- The multi-string has the highest RE penetration but also has the highest curtailment.
- The AC module has the lowest curtailment and LPSP but has the lowest RE penetration. The addition of batteries can increase the RE size the largest.

VI. CONCLUSION

This paper has studied the effect of using different types of inverters in the sizing of the DG-PV and DG-PV systems considering cost and uncertainties. This paper has proven that due to the difference in technical specifications of different inverter types, the sizing consideration is also affected. Furthermore, considering different criteria, such as least COE, least LPSP, optimality, RE penetration, curtailment, and changes in equipment costs affects the choice between inverters.

Future studies can be done with this model by changing the EMS of the system, where a conventional rule-based approach was used. This may involve some control strategies or co-optimization of the dispatch of each system component. Though this would increase the complexity of the problem by turning it to a multi-layer optimization, the flexibility of the design increases as there would be more options for the dispatch to move in order to find a more optimal result. Furthermore, other problems in high penetration renewable energy may be studied such as stability and power quality.

REFERENCES

[1] K. Lappalainen and S. Valkealahti, "Output power variation of different PV array configurations during irradiance transitions caused by moving clouds," *Appl. Energy*, vol. 190, pp. 902–910, Mar. 2017, doi: 10.1016/j.apenergy.2017.01.013.

[2] K. Lappalainen and S. Valkealahti, "Analysis of shading periods caused by moving clouds," *Sol. Energy*, vol. 135, pp. 188–196, Oct. 2016, doi: 10.1016/j.solener.2016.05.050.

[3] J. Väisänen, A. Kosonen, J. Ahola, T. Sallinen, and T. Hannula, "Optimal sizing ratio of a solar PV inverter for minimizing the levelized cost of electricity in Finnish irradiation conditions," *Sol. Energy*, vol. 185, pp. 350–362, Jun. 2019, doi: 10.1016/j.solener.2019.04.064.

[4] T. E. K. Zidane, M. R. B. Adzman, M. F. N. Tajuddin, S. M. Zali, and A. Durusu, "Optimal configuration of photovoltaic power plant using grey wolf optimizer: A comparative analysis considering CdTe and c-Si PV modules," *Sol. Energy*, vol. 188, pp. 247–257, Feb. 2019, doi: 10.1016/j.solener.2019.06.002.

[5] M. Gharibi and A. Askarzadeh, "Size optimization of an off-grid hybrid system composed of photovoltaic and diesel generator subject to load variation factor," *J. Energy Storage*, vol. 25, Oct. 2019, Art. no. 100814, doi: 10.1016/j.est.2019.100814.

[6] N. Ghorbani, A. Kasaeian, A. Toopshekan, L. Bahrami, and A. Maghami, "Optimizing a hybrid wind-PV-battery system using GA-PSO and MOPSO for reducing cost and increasing reliability," *Energy*, vol. 154, pp. 581–591, Jul. 2018, doi: 10.1016/j.energy.2017.12.057.

[7] S. Bandyopadhyay, G. R. C. Mouli, Z. Qin, L. R. Elizondo, and P. Bauer, "Techno-economical model based optimal sizing of PV-battery systems for microgrids," *IEEE Trans. Sustain. Energy*, vol. 11, no. 3, pp. 1657–1668, Jul. 2020, doi: 10.1109/TSTE.2019.2936129.

[8] M. N. Ashtiani, A. Toopshekan, F. R. Astaraei, H. Yousefi, and A. Maleki, "Techno-economic analysis of a grid-connected PV/battery system using the teaching-learning-based optimization algorithm," *Sol. Energy*, vol. 203, pp. 69–82, Jun. 2020, doi: 10.1016/j.solener.2020.04.007.

[9] B. K. Das and F. Zaman, "Performance analysis of a PV/diesel hybrid system for a remote area in Bangladesh: Effects of dispatch strategies, batteries, and generator selection," *Energy*, vol. 169, pp. 263–276, Feb. 2019, doi: 10.1016/j.energy.2018.12.014.

[10] T. Salameh, C. Ghenai, A. Merabet, and M. Alkasrawi, "Techno-economical optimization of an integrated stand-alone hybrid solar PV tracking and diesel generator power system in Khorfakkan, United Arab Emirates," *Energy*, vol. 190, Jan. 2020, Art. no. 116475, doi: 10.1016/j.energy.2019.116475.

[11] A. L. Bukar, C. W. Tan, and K. Y. Lau, "Optimal sizing of an autonomous photovoltaic/wind/battery/diesel generator microgrid using grasshopper optimization algorithm," *Sol. Energy*, vol. 188, pp. 685–696, Aug. 2019, doi: 10.1016/j.solener.2019.06.050.

[12] A. Fathy, K. Kaaniche, and T. M. Alanazi, "Recent approach based social spider optimizer for optimal sizing of hybrid PV/wind/battery/diesel integrated microgrid in aljouf region," *IEEE Access*, vol. 8, pp. 57630–57645, 2020, doi: 10.1109/ACCESS.2020.2982805.

[13] A. A. Z. Diab, H. M. Sultan, I. S. Mohamed, O. N. Kuznetsov, and T. D. Do, "Application of different optimization algorithms for optimal sizing of PV/wind/diesel/battery storage stand-alone hybrid microgrid," *IEEE Access*, vol. 7, pp. 119223–119245, 2019, doi: 10.1109/ACCESS.2019.2936656.

[14] A. Q. Mohammed, K. A. Al-Anbarri, and R. M. Hannun, "Optimal combination and sizing of a stand–alone hybrid energy system using a nomadic people optimizer," *IEEE Access*, vol. 8, pp. 200518–200540, 2020, doi: 10.1109/ACCESS.2020.3034554.

[15] U. Akram, M. Khalid, and S. Shafiq, "An improved optimal sizing methodology for future autonomous residential smart power systems," *IEEE Access*, vol. 6, pp. 5986–6000, 2018, doi: 10.1109/ACCESS.2018.2792451.

[16] F. Nejabatkhah, Y. W. Li, A. B. Nassif, and T. Kang, "Optimal design and operation of a remote hybrid microgrid," *CPSS Trans. Power Electron. Appl.*, vol. 3, no. 1, pp. 3–13, Mar. 2018, doi: 10.24295/CPSSTPEA.2018.00001.

[17] D. Yang, C. Jiang, G. Cai, and N. Huang, "Optimal sizing of a wind/solar/battery/diesel hybrid microgrid based on typical scenarios considering meteorological variability," *IET Renew. Power Gener.*, vol. 13, no. 9, pp. 1446–1455, Jul. 2019. [Online]. Available: https://digital-library.theiet.org/content/journals/10.1049/iet-rpg.2018.5944

[18] S. K. Sahoo, S. Sukchai, and F. F. Yanine, "Review and comparative study of single-stage inverters for a PV system," *Renew. Sustain. Energy Rev.*, vol. 91, pp. 962–986, Aug. 2018, doi: 10.1016/j.rser.2018.04.063.

[19] R. Dogga and M. K. Pathak, "Recent trends in solar PV inverter topologies," *Sol. Energy*, vol. 183, pp. 57–73, May 2019, doi: 10.1016/j.solener.2019.02.065.

[20] K. Zeb, W. Uddin, M. A. Khan, Z. Ali, M. U. Ali, N. Christofides, and H. J. Kim, "A comprehensive review on inverter topologies and control strategies for grid connected photovoltaic system," *Renew. Sustain. Energy Rev.*, vol. 94, pp. 1120–1141, Oct. 2018, doi: 10.1016/j.rser.2018.06.053.

[21] M. S. Tariq, S. A. Butt, and H. A. Khan, "Impact of module and inverter failures on the performance of central-, string-, and micro-inverter PV systems," *Microelectron. Rel.*, vols. 88–90, pp. 1042–1046, Sep. 2018.

[22] D. Feldman, V. Ramasamy, R. Fu, A. Ramdas, J. Desai, and R. Margolis, "U.S. solar photovoltaic system cost benchmark: Q1," Nat. Renew. Energy Lab., Golden, CO, USA, Tech. Rep. NREL/TP-6A20-77324, 2021. [Online]. Available: https://www.nrel.gov/docs/fy21osti/77324.pdf

[23] M. A. M. Ramli, H. R. E. H. Bouchekara, and A. S. Alghamdi, "Optimal sizing of PV/wind/diesel hybrid microgrid system using multi-objective self-adaptive differential evolution algorithm," *Renew. Energy*, vol. 121, pp. 400–411, Jan. 2018, doi: 10.1016/j.renene.2018.01.058.

[24] M. Alanazi, M. Mahoor, and A. Khodaei, "Co-optimization generation and transmission planning for maximizing large-scale solar PV integration," *Int. J. Electr. Power Energy Syst.*, vol. 118, Jun. 2020, Art. no. 105723, doi: 10.1016/j.ijepes.2019.105723.

[25] R. Wang, Q. Sun, P. Tu, J. Xiao, Y. Gui, and P. Wang, "Reduced-order aggregate model for large-scale converters with inhomogeneous initial conditions in DC microgrids," *IEEE Trans. Energy Convers.*, vol. 36, no. 3, pp. 2473–2484, Sep. 2021, doi: 10.1109/TEC.2021.3050434.

[26] M. Chankaya, I. Hussain, and A. Ahmad, "AdaGrad based control for grid-tied PV battery fuel cell system," in *Proc. IEEE Students Conf. Eng. Syst. (SCES)*, Jul. 2020, pp. 1–6, doi: 10.1109/SCES50439.2020.9236739.

[27] *MERRA-2 Meteorological Re-Analysis*, SoDA: Solar radiation Data, Mines ParisTech and Transvalor S.A, Paris, France. Accessed: 2020.

[28] A. Gupta, R. P. Saini, and M. P. Sharma, "Modelling of hybrid energy system—Part I: Problem formulation and model development," *Renew. Energy*, vol. 36, no. 2, pp. 459–465, Feb. 2011.

[29] E. Ocampo, Y.-C. Huang, and C.-C. Kuo, "Feasible reserve in day-ahead unit commitment using scenario-based optimization," *Energies*, vol. 13, no. 20, p. 5239, Oct. 2020. [Online]. Available: https://www.mdpi.com/1996-1073/13/20/5239

[30] W. Cole and A. W. Frazier, "Cost projections for utility-scale battery storage: 2020 update," Nat. Renew. Energy Lab., Golden, CO, USA, Tech. Rep., NREL/TP-6A20-75385, 2020. [Online]. Available: https://www.nrel.gov/docs/fy20osti/75385.pdf

ERICA M. OCAMPO received the B.S. degree in electrical engineering from the University of Santo Tomas (UST), Manila, Philippines, in 2008, and the M.S. degree in electrical engineering from the National Taiwan University of Science and Technology (NTUST), Taipei, Taiwan, in 2018. She is currently pursuing the Ph.D. degree in electrical engineering with Taiwan Tech.

From 2009 to 2019, she was affiliated with UST, as an Instructor with the Faculty of Engineering and a Research Staff in a project with the Department of Science and Technology. Her research interests include optimal power flow and application of machine learning and artificial intelligence in power systems.

WEN-CHING CHANG was born in Taoyuan, Taiwan, in July 1995. He received the M.S. degree from the National Cheng Kung University, in 2019. He is currently pursuing the Ph.D. degree with the National Taiwan University of Science and Technology. His research interests include finite element analysis, medium-voltage solid-state transformer, and maximum power point tracker.

CHENG-CHIEN KUO was born in Yunlin, Taiwan, in August 1969. He received the B.S., M.S., and Ph.D. degrees from the National Taiwan University of Science and Technology (NTUST), in 1991, 1993, and 1998, respectively. He was with St. John's University, from 1994 to 2015. Since 2015, he has been with NTUST, where he is currently a Professor and the Assistant Head of the Department of Electrical Engineering. His research interests include fault diagnosis, conditional monitoring system design, distribution automation, partial discharge measurement, and optimization techniques.